doi:10.1093/brain/awr104 Brain 2011: 134; 1658–1672 | 1658

BRAIN
A JOURNAL OF NEUROLOGY

β-amyloid activates PARP causing astrocytic metabolic failure and neuronal death

Rosella Abeti,[1] Andrey Y. Abramov[2,*] and Michael R. Duchen[1,*]

1 Department of Cell and Developmental Biology and UCL Consortium for Mitochondrial Research, University College London, London WC1E 6BT, UK
2 Department of Molecular Neuroscience, UCL Institute of Neurology, London WC1N 3BG, UK

*These authors contributed equally to this work.

Correspondence to: Dr Andrey Y. Abramov,
Department of Molecular Neuroscience,
UCL Institute of Neurology,
Queen Square,
London WC1N 3BG, UK
E-mail: a.abramov@ucl.ac.uk

Alzheimer's disease is characterized by β-amyloid accumulation in the central nervous system. As β-amyloid is neurotoxic in culture, we have explored the mechanisms of toxicity in the search for therapeutic targets for Alzheimer's disease and now identify a key role for poly(ADP-ribose) polymerase in β-amyloid-induced neuronal death. Exposure of hippocampal neuronal/glial co-cultures to β-amyloid peptides activates the glial nicotinamide adenine dinucleotide phosphate oxidase, followed by predominantly neuronal cell death. β-amyloid exposure caused the progressive loss of mitochondrial membrane potential in astrocytes, accompanied by transient mitochondrial depolarizations caused by reversible openings of the mitochondrial permeability transition pore. The transients were absent in cultures from cyclophilin D knockout mice, leaving the slow depolarization available for study in isolation. β-amyloid exposure decreased both nicotinamide adenine dinucleotide fluorescence and oxygen consumption, while provision of mitochondrial substrates reversed the depolarization, suggesting that substrate supply was limiting. Poly(ADP-ribose) polymerase is activated by oxidative stress and consumes nicotinamide adenine dinucleotide, decreasing substrate availability. β-amyloid exposure caused accumulation of the poly(ADP-ribose) polymerase product, poly-ADP-ribose polymers, in astrocytes. Inhibition of either poly(ADP-ribose) polymerase or of the nicotinamide adenine dinucleotide phosphate oxidase prevented the appearance of poly-ADP-ribose polymers and the mitochondrial depolarization. Exposure of co-cultures to β-amyloid for >8 h decreased nicotinamide adenine dinucleotide and mitochondrial membrane potential and increased cell death in neurons, all of which were prevented by poly(ADP-ribose) polymerase inhibitors. Poly-ADP-ribose polymers increased with age in the brains of the TASTPM Alzheimer mouse model. We conclude that β-amyloid-induced neuronal death is mediated by poly(ADP-ribose) polymerase in response to oxidative stress generated by the astrocytic nicotinamide adenine dinucleotide phosphate oxidase.

Keywords: amyloid; PARP; mitochondria; reactive oxygen production; NADPH oxidise

Abbreviations: $\Delta\psi_m$ = mitochondrial membrane potential; PAR = poly(ADP ribose); PARP = poly(ADP-ribose) polymerase

Received November 5, 2010. Revised March 26, 2011. Accepted March 28, 2011

Introduction

Alzheimer's disease is the most common cause of dementia. The characteristic histological features of the post-mortem brain of patients with Alzheimer's disease are senile plaques and neurofibrillary tangles—the two pathological markers required to make a definitive diagnosis of Alzheimer's disease (Wilcock and Esiri, 1982). Neurofibrillary tangles are formed from filamentous aggregates of hyperphosphorylated tau protein (Pelech, 1995), while the senile plaques consist of insoluble extracellular aggregates of different isoforms (39–42 amino acids) of β-amyloid peptide (Masters *et al.,* 1985; Hardy and Selkoe, 2002). Accumulating evidence suggests that β-amyloid peptides represent a major component of the pathophysiology of neurodegeneration in Alzheimer's disease, although the mechanisms remain controversial.

Mitochondrial dysfunction has been identified as a very early feature of the pathology, appearing even before neurofibrillary tangles can be found (Hirai *et al.,* 2001). It has been proposed that β-amyloid may directly influence mitochondrial function. Direct exposure even of isolated mitochondria to β-amyloid impairs the activity of enzyme complexes of the respiratory chain, such as α-ketoglutarate dehydrogenase and aconitase (Blass and Gibson, 1991; Casley *et al.,* 2002), increases mitochondrial production of reactive oxygen species (Sheehan *et al.,* 1997) and may induce opening of the mitochondrial permeability transition pore (Parks *et al.,* 2001; Shevtzova *et al.,* 2001).

We have found that exposure of mixed primary neuronal/glial cultures to β-amyloid causes a rise in intracellular-free calcium ($[Ca^{2+}]_c$) in astrocytes, but not in neurons. This was associated with a calcium-dependent increase in the generation of reactive oxygen species (Abramov *et al.,* 2003, 2004*a*, *b*), which was in turn associated with a slow and progressive dissipation of mitochondrial membrane potential ($\Delta\psi_m$) on which abrupt calcium-dependent transient mitochondrial depolarizations were superimposed (Abramov *et al.,* 2004*a*, *b*). The progressive loss of $\Delta\psi_m$ was reversed by exposure to substrates for mitochondrial complex I (malate and glutamate, pyruvate), complex II (methyl succinate) and complex IV (N,N,N′,N′-Tetramethyl-p-Phenylenediamine [TMPD] and ascorbate) (Abramov *et al.,* 2004*b*) suggesting that it reflects impaired mitochondrial substrate supply. The substrates had no effect at all on the transient depolarizations, suggesting that these reflect an independent process. Both reactive oxygen species generation and the mitochondrial response were prevented by pharmacological or genetic inhibition of the NADPH oxidase. Together, these data suggest that the mitochondrial depolarization reflects oxidative damage to metabolic pathways upstream of mitochondrial complex I (Abramov *et al.,* 2004*a,* 2005). The combination of β-amyloid-induced oxidative stress and the changes in $[Ca^{2+}]_c$ cause large but reversible transient mitochondrial depolarizations that were prevented by pretreatment with cyclosporin A and by free radical scavengers, suggesting that these reflect transient openings of the mitochondrial permeability transition pore, in itself a remarkable and unusual observation. The mechanism of the reactive oxygen species-induced progressive mitochondrial depolarization remains unclear. In particular, the link between oxidative stress following activation of the NADPH oxidase and impaired substrate supply for mitochondrial respiration in astrocytes remains obscure.

One possible mechanism of β-amyloid-induced mitochondrial depolarization could involve upregulation of the activity of the DNA repair protein poly(ADP-ribose) polymerase (PARP) in response to oxidative damage to DNA, as this can cause depletion of NAD^+ (Diefenbach and Burkle, 2005; Abramov and Duchen, 2008). The PARP family includes 18 members; however, 90% of poly(ADP ribose) polymers (PARs) are synthesized by PARP-1, and we will consider only this enzyme (Burkle, 2005; Moroni, 2008). The presence of PAR polymers has been demonstrated in post-mortem material in the brains of patients with Alzheimer's disease (Love *et al.,* 1999) and in skin fibroblasts and lymphoblasts from patients with Alzheimer's disease (Cecchi *et al.,* 2002). Furthermore, β-amyloid has been shown to inhibit glucose uptake in cultured neurons and astrocytes (Keller *et al.,* 1997; Parpura-Gill *et al.,* 1997; Uemura and Greenlee, 2001), a mechanism that could also restrict the availability of substrates for respiratory complexes.

We have previously shown that although the short-term consequences of β-amyloid exposure seem restricted to glial cells—astrocytes and microglia—this is followed later by oxidative stress, glutathione depletion and death of neurons (Abramov *et al.,* 2003, 2004*a*). Neurons were rescued by glutathione precursors, genetic or chemical inhibition of the NADPH oxidase, and by anti-oxidant scavengers, placing oxidative stress following activation of the NADPH oxidase centre stage in the mechanism of β-amyloid neurotoxicity. In the present study, we sought to clarify the specific mechanism that leads from oxidative stress in astrocytes to neuronal death.

Materials and methods

Peptides and treatments

β-amyloid$_{25–35}$ and β-amyloid$_{1–42}$ (Bachem) were dissolved at 1 mM in sterile hypertonic sodium bicarbonate solution (Invitrogen) and kept frozen until use. The peptides were added under the microscope, except for neurotoxicity measurements, where they were added 24 h before the experiment. β-Amyloid$_{1–42}$ was used at concentration of 5 μM and β-amyloid$_{25–35}$ was used at concentrations of up to 50 μM in order to ensure that the peptides were present in molar excess compared with inhibitors and so exclude any direct interaction. We emphasize that for all experiments presented here and in a long series of experiments published over the last 7 years, all responses are equivalent for the 1–42 and 25–25 peptides and the two are used interchangeably. Control experiments to the reverse peptide 35–25 have never shown any significant responses.

Cell culture

Mixed cultures of hippocampal neurons and glial cells were prepared as described previously (Abramov *et al.,* 2004*a*) with modifications, from Sprague-Dawley rat pups 2–4 days post-partum (UCL breeding colony). For some experiments, cyclophilin D knockout transgenic mice (obtained as a kind gift from J. D.Molkentin, Cincinnati Children's Hospital Medical School) were used and B6/cv129 6 pups (the strain used as a background for the transgenic animals) were used as

controls. Hippocampi were removed into ice-cold HEPES-buffered salt solution (Ca^{2+}, Mg^{2+}-free; Invitrogen). The tissue was minced and trypsinized (0.1% for 15 min at 37°C), triturated and plated onto poly-D-lysine-coated coverslips and cultured in neurobasal medium (Invitrogen) supplemented with B-27 (Invitrogen) and 2 mM L-glutamine. Cultures were maintained at 37°C in a humidified atmosphere of 5% CO_2 and 95% air, fed twice a week and maintained for a minimum of 10 days before experimental use to ensure the expression of glutamate and other receptors. Neurons were easily distinguishable from glia: they appeared phase bright, had smooth rounded somata and distinct processes, and lay just above the focal plane of the glial layer. Cells were used at 10–15 days *in vitro* unless stated differently.

Immunocytochemistry

Primary co-cultures of hippocampal neurons and astrocytes were treated with 50 μM of β-amyloid$_{25–35}$ or 1 μg/ml of phorbol 12-myristate 13-acetate (PMA) for 1 h. Inhibitors 3-aminobenzamide (1 mM) or diphenylene iodonium (0.5 μM) were used 20 min before and during exposure to β-amyloid where appropriate. Cells grown on coverslips were fixed with ice-cold 4% (v/v) formaldehyde in phosphate-buffered saline (0.2 M Na_2HPO_4 adjusted with 0.2 M NaH_2PO_4 to pH 7.4) for 30 min and subsequently permeabilized for 15 min using 0.5% (v/v) Triton X-100 in phosphate-buffered saline. After a blocking step with complete medium for 1 h at room temperature, the cells were incubated with primary antibodies. PAR polymers were detected using a monoclonal 10 H L-PAR 1:2 (a gift from Mathias Ziegler, University of Bergen). Neurons and astrocytes were identified using rabbit glial fibrillary acidic protein (1:500, Abcam) or rabbit neurofilament (1:500, Sigma) diluted in complete medium for 1 h at room temperature. Cells were washed with phosphate-buffered saline, followed by 1 h incubation with the secondary antibody at room temperature, anti-mouse FITC (1:600) and anti-rabbit Cy3 (1:250) in complete medium. Coverslips were mounted with Vectashield mounting medium and with DAPI to stain the nuclei.

Immunohistochemistry

Double transgenic mice TASTPM, generated with the human APP Swedish mutation (TAS10 mice) and the human presenilin 1 M146V mutation (TPM mice) (Howlett, 2004), were culled. Brains were quickly removed and placed in ice-cold CSF containing (in millimolars): 125 NaCl, 3.5 KCl, 25 $NaHCO_3$, 1.25 Na_2HPO_4, 1.5 $CaCl_2$, 1 $MgCl_2$, 25 glucose and 0.5 Na-ascorbate (pH 7.4 with 95% O_2/5% CO_2). Slices were cut using an HR2 Slicer (Sigman Electronic) at 100-μm thickness, and were transferred to a solution of 4% paraformaldehyde in phosphate-buffered saline. After 5 h the slices were washed three times in phosphate-buffered saline, and permeabilized in 0.5% (v/v) Triton X-100 for 30 min at room temperature followed by three washes in phosphate-buffered saline. Slices were incubated for 1 h in a blocking solution of 10% goat serum, 3% bovine serum albumin and 0.01% of Tween-20 in phosphate-buffered saline. After blocking the slices were incubated with primary antibodies (1 h at room temperature). PAR polymers were detected with mouse α-PAR (Axxora) and neurons or astrocytes were labelled with chicken α-MAP-2 (Abcam) and rabbit α-glial fibrillary acidic protein (Abcam), respectively. Suitable secondary antibodies were then applied. Slices were washed and incubated with a 10 μM Hoescht solution for 10 min at room temperature, to stain the nuclei. After further washing the slices were mounted on glass slides with Vectashield mounting medium and coverslips applied on top of each slice. The secondary antibodies used were: goat α-chicken FITC (1:500, Abcam), goat α-mouse Cy3 (1:500, Abcam) and donkey α-rabbit FITC (1:500, Abcam) or goat α-rabbit Cy3 (1:200, Jackson). Images were acquired on a Zeiss 700 microscope.

Western blot analysis

Brain tissues were obtained, from TASTPM mice and the matched wild-type, in accordance with the UK Home Office Animals (Scientific Procedures) and freshly placed into radioimmunoprecipitation lysis buffer [50 mM Tris–HCl, pH 7,4, 1% (v/v) nonidet P-40, 150 mM NaCl, 0.25% deoxycholate, 1 mM ethylenediaminetetraacetic acid (EDTA), 1 mM phenylmethylsulphonylfluoride (PMSF), 1 mM Na_3VO_4, 1 mM NaF and 1 tablet of protease inhibitor cocktail for 10 ml of solution], and homogenized with Ultra-Turrax homogenizer. The samples were centrifuged at 25 000 *g* for 20 min at 4°C. The supernatant was then mixed with 2× Laemmli buffer. Samples were subjected to sodium dodecyl sulphate polyacrylamide gel electrophoresis and western blotting according to standard procedures. Blots were developed with rabbit polyclonal p40-phox phospho (1/1000; Cell Signalling) and mouse monoclonal α-Tubulin (Sigma). Peroxidase-conjugated secondary antibodies were enhanced by chemiluminescence (ECL-Advanced; Amersham Biosciences) and detected by ChemiDoc XRS + System (Bio-Rad).

Imaging $[Ca^{2+}]_c$, mitochondrial membrane potential and 2-NBDG

Cells were loaded for 30 min at room temperature with 5 μM fura-2 AM (Molecular Probes) and 0.005% Pluronic in a HEPES-buffered salt solution composed (millimolars): 156 NaCl, 3 KCl, 2$MgSO_4$, 1.25 KH_2PO_4, 2 $CaCl_2$, 10% glucose and 10% HEPES, pH adjusted to 7.35 with NaOH. For simultaneous measurement of $[Ca^{2+}]_c$ and $\Delta\psi_m$, Rh123 (10 μM; Molecular Probes) was added into the cultures during the last 15 min of the fura-2 loading period. Fluorescence measurements were obtained on an epifluorescence inverted microscope equipped with a ×20 fluorite objective. $[Ca^{2+}]_c$ and $\Delta\psi_m$ were monitored in single cells using excitation light provided by a Xenon arc lamp, using a monochromator (Cairn Research) to excite fluorescence sequentially at 340, 380 and 490 nm (all at 10 nm bandwidth). Emitted fluorescence light was reflected by a 515 nm long-pass filter to a frame transfer cooled CCD camera (Hamamatsu Orca ER). All imaging data were collected and analysed using software from Andor. The fluorescence data were acquired at intervals of 10 s. The fura-2 data have not been calibrated in terms of $[Ca^{2+}]_c$ because of the uncertainty arising from the use of different calibration techniques. Accumulation of Rh123 in polarized mitochondria quenches the fluorescent signal, and in response emission is dequenched; an increase in Rh123 signal therefore signals mitochondrial depolarization. For glucose uptake experiments, the uptake of the fluorescent glucose homologue 2-(*N*-(7-nitrobenz-2-oxa-1,3-diazol-4-yl)amino)-2-deoxyglucose (2-NBDG; Invitrogen) was measured by the addition of 2 μM 2-NBDG in the presence of 0.25 mM glucose during a period of continuous imaging. 2-NDBG was excited at 458 nm and fluorescence was measured at 520 nm. All presented data were obtained from at least five coverslips and two to three different cell preparations.

Measurement of NAD(P)H autofluorescence

The autofluorescence of NADH [and NADPH and so we will refer to this as NAD(P)H] in co-cultures of neurons and astrocytes was imaged

on a Zeiss 510 META UV-VIS confocal microscope. The blue autofluorescence emitted by the pyridine nucleotides NADH and NADPH in their reduced form was excited with a UV laser (Coherent; at 351 nm) and emission was collected using a 435–485 nm band pass filter. To measure the dynamic range of the signal in relation to the full mitochondrial NADH pool and to normalize the data, the maximum oxidation and maximum reduction, cells were exposed to carbonyl cyanide 4-(trifluoromethoxy) phenylhydrazone (FCCP, 1 μM—to stimulate respiration and achieve maximum NADH oxidation) and NaCN (1 mM—to inhibit respiration and achieve maximum NADH reduction).

The final formula used to normalize the NADH autofluorescence measurements was:

$$(F - F_{fccp})/(F_{cn} - F_{fccp})$$

Quantitative analysis of the images obtained was done using the Zeiss LSM 510 software.

Oxygen consumption measurement

To measure respiration rate in intact cells $\sim 1 \times 10^7$ cells were suspended in respiration medium (HEPES-buffered salt solution) with 10 mM D-glucose in a Clark-type oxygen electrode thermostatically maintained at 37°C. The oxygen electrode was calibrated with air-saturated water, assuming 406 nmol O atoms/ml at 37°C (Oxytherm system, Hansatech Instruments). The rate of oxygen consumption was measured 10 min after application of β-amyloid$_{25–25}$ (50 μM). At the end of every experiment FCCP (0.5 μM) was added to establish maximal uncoupled respiratory rate.

Cell death

Cells were incubated with propidium iodide (10 μM) and Hoechst 33258 (1 μg/μl) for 15 min, washed three times with HEPES-buffered salt solution and analysed using an epifluorescence inverted microscope equipped with a ×20 fluorite objective. Hoechst 33258 stains all nuclei while propidium iodide only stains cells with a disrupted plasma membrane. Dead cells (propidium iodide positive), were counted as a fraction of neurons or astrocytes. Neurons were identified using phase-contrast optics: they are readily distinguishable from the flatter astrocytes and lay in a different focal plane, above the glial layer. In each experiment, ~200 cells were examined in four random fields from three or more culture wells for each condition.

Statistical analysis

Statistical analysis was performed with the aid of Origin 8 (Microcal Software Inc.) software. Results are expressed as means ± standard error of the mean (SEM). The ANOVA test was employed when appropriate and the point of minimum acceptable statistical significance was taken to be 0.05, and was Bonferroni corrected where required.

Results

β-amyloid exposure and activation of the NADPH oxidase induce changes in $\Delta\psi_m$ in astrocytes

We have previously shown that application of the β-amyloid peptide fragment 25–35 (5–50 μM) or the full-length peptide 1–42 (0.5–5 μM) to rat or mouse hippocampal neurons and astrocytes in co-culture causes sporadic increases in intracellular calcium ($[Ca^{2+}]_c$) and complex changes in $\Delta\psi_m$ in astrocytes, while both $[Ca^{2+}]_c$ and $\Delta\psi_m$ remain stable in adjacent neurons (Abramov *et al.*, 2004*a*). Figure 1A illustrates the nature of the β-amyloid-induced changes in $\Delta\psi_m$ in astrocytes. This response consists of two components: (i) a reactive oxygen species-dependent (Abramov *et al.*, 2004*a*), slowly progressive mitochondrial depolarization; and (ii) Ca^{2+}- and reactive oxygen species-dependent, large, transient and reversible abrupt mitochondrial depolarizations, which are superimposed on the slow progressive depolarization (Abramov *et al.*, 2004*a*) and which coincide with changes in $[Ca^{2+}]_c$ (Fig. 1A) (Abramov *et al.*, 2004*a*). Both β-amyloid-induced changes in intracellular $[Ca^{2+}]_c$ and the transient mitochondrial depolarizations are dependent on influx of extracellular Ca^{2+} (Abramov *et al.*, 2004*a*). However, β-amyloid-induced reactive oxygen species production by the NADPH oxidase is required to initiate both components of the changes in $\Delta\psi_m$ of astrocytes, as both pharmacological and genetic inhibition of this enzyme completely prevented the depolarizations (Abramov *et al.*, 2004*a*, 2005). Consistent with this model, the phorbol ester PMA (1 μg/ml), an activator of the NADPH oxidase, also caused a slow progressive loss of $\Delta\psi_m$ in hippocampal astrocytes (Fig. 1B, $n = 114$ astrocytes, $n = 3$ experiments), which was prevented by pre-treatment with the NADPH oxidase inhibitor, diphenylene iodonium (0.5 μM) (Fig. 1C, $n = 99$ astrocytes, $n = 3$ experiments). Thus activation of the NADPH oxidase appears to be sufficient to induce the progressive loss of mitochondrial membrane potential.

Calcium overload and reactive oxygen species signalling converge on the mitochondria as triggers that open the mitochondrial permeability transition pore (for reviews see Crompton *et al.*, 2002; Rasola and Bernardi, 2007). We have previously shown that the transient mitochondrial depolarizations, but not the slower depolarization, are blocked by cyclosporin A (Abramov *et al.*, 2004*a*) and so we used cultures prepared from transgenic mice in which cyclophilin D was knocked out (generously provided by J. D. Molkentin) in order to isolate and study the slower depolarization. Cyclophilin D is an essential regulator of mitochondrial permeability transition pore opening and mitochondrial permeability transition pore opening is suppressed in tissues from these animals (Baines *et al.*, 2005). The effects of β-amyloid on $\Delta\psi_m$ in astrocytes cultured from control mice were indistinguishable from the effects on primary astrocytes from rats. When β-amyloid$_{1–42}$ (5 μM) was applied to co-cultures of hippocampal neurons and astrocytes from cyclophilin D knockout mice, the large transient changes in $\Delta\psi_m$ normally induced by β-amyloid were absent (Fig. 1D: $n = 125$ cells, $n = 3$ experiments), confirming that these events represent transient and reversible openings of the mitochondrial permeability transition pore. Curiously, the slowly progressive mitochondrial depolarization seen in response to β-amyloid in these cells was significantly faster than that recorded in cells from matched controls, with an average increase in Rh123 signal after 20 min β-amyloid-exposure of 79.4 ± 6.1% compared with 47.6 ± 3.6% in those of control mouse hippocampal astrocytes, which showed only a slow depolarization ($n = 78$ of mouse control astrocytes, $P < 0.05$).

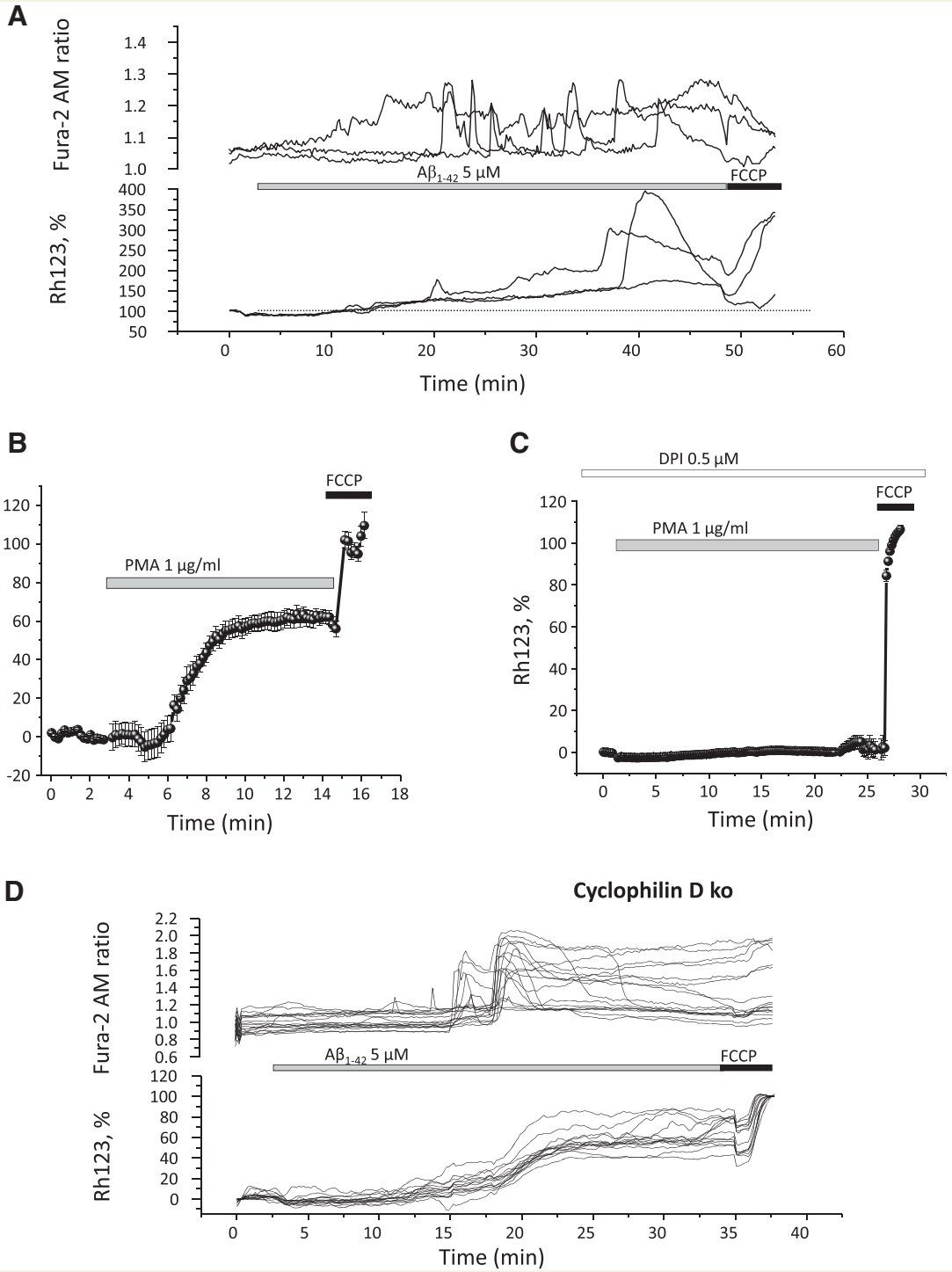

Figure 1 β-amyloid causes mitochondrial depolarization in astrocytes. Changes in $\Delta\psi_m$ and in $[Ca^{2+}]_c$ with time were measured using Rh 123 in 'dequench' mode (where the loss of potential is seen as an increase in fluorescence) and fura-2 AM, respectively. (**A**) Changes in $[Ca^{2+}]_c$ (*top*) and $\Delta\psi_m$ (*bottom*) in astrocytes (each trace represents a single cell where three cells reproduce three different types of depolarization) following exposure to 5 μM β-amyloid$_{1–42}$. (**B**) Application of PMA (1 μg/ml, trace represent the mean values of all the cells of single experiment), an activator of the NADPH oxidase, also induced a slow mitochondrial depolarization in astrocytes that was prevented by inhibition of the NADPH oxidase using 0.5 μM diphenylene iodonium (**C**). (**D**) The effect of the full peptide β-amyloid$_{1–42}$ (5 μM) on cortical astrocytes (traces from individual cells) from cyclophilin D knockout mice, in which the cells responded to β-amyloid with only a slow progressive loss of $\Delta\psi_m$. The transient depolarizations were not seen in this preparation.

Acute exposure to β-amyloid causes oxidation of the mitochondrial NADH pool in astrocytes

If the loss of $\Delta\psi_m$ is due to impaired mitochondrial substrate supply, as suggested by the restoration of potential by mitochondrial substrates, pyruvate methyl succinate or N,N,N′,N′-Tetramethyl-p-Phenylenediamine/ascorbate (Abramov *et al.*, 2004*a*), it seemed possible that the cells were becoming depleted of NADH. We therefore examined changes in UV-induced blue autofluorescence, which mostly arises from mitochondrial NADH (Chance, 1976). Application of 5 μM β-amyloid$_{1–42}$ caused a large and highly significant progressive decrease in NAD(P)H fluorescence of hippocampal astrocytes following a delay of ~5 min, such that the autofluorescence signal fell by 32 ± 2.1% in 20 min (n = 101). Activation of respiration with the uncoupler FCCP (1 μM) causing maximal oxidation of NAD(P)H, in order to reduce the fluorescence signal to a minimal level, only reduced the fluorescence signal by a further 7.1 ± 0.63% (n = 101) (in control astrocytes, FCCP decreased NADH signal by 44.5 ± 4.1%, n = 56), suggesting that most of the NADH was already either depleted or oxidized. Subsequent inhibition of the respiratory chain with NaCN (1 mM), which prevents oxidation of NAD(P)H by complex I, increased the autofluorescence signal to its maximal

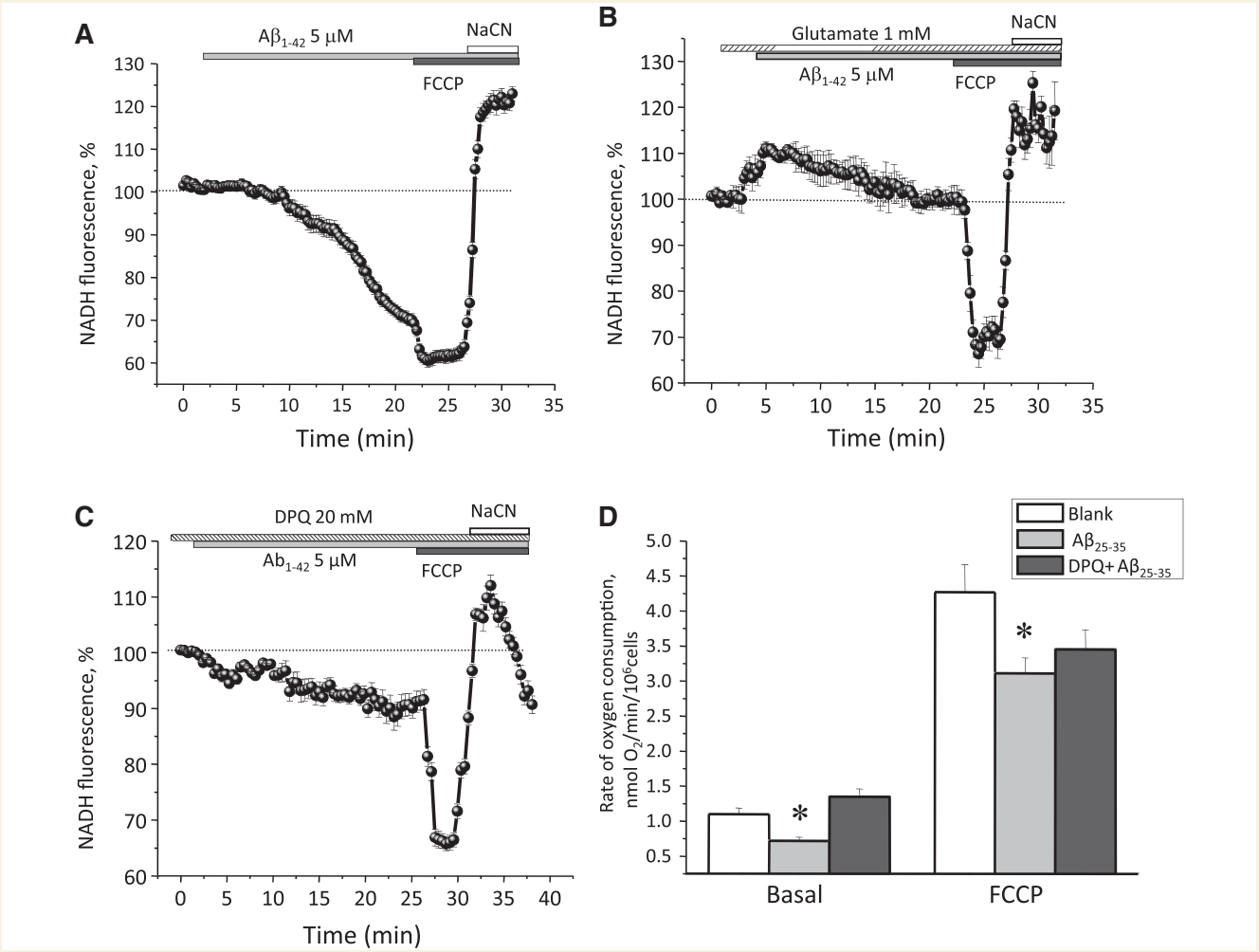

Figure 2 β-amyloid decreases NADH autofluorescence and reduces mitochondrial oxygen consumption in hippocampal astrocytes. (**A**) Application of 5 μM β-amyloid$_{1–42}$ caused a slow, progressive decrease in the NADH autofluorescence signal (shown as the averaged response from 35 cells) in hippocampal astrocytes. Note that the response to FCCP (1 μM) was very small at the end of this recording period, while the response to 1 mM NaCN (CN^-) restored the original signal, suggesting that the NADH pool was nearly fully oxidized. (**B–C**) The response to β-amyloid was prevented in cells pre-incubated with the mitochondrial substrate glutamate (1 mM) or with the PARP inhibitor 3,4-Dihydro-5[4-(1-piperindinyl)butoxy]-1(2H)-isoquinoline (DPQ) (20 μM). (**D**) The rate of oxygen consumption was measured from astrocytes in suspension using a Clarke electrode. Mitochondrial respiration was significantly reduced following pretreatment of cells with 50 μM β-amyloid$_{25–35}$ for 10 min. The maximal rate of respiration, induced by FCCP (1 μM) was also significantly reduced in β-amyloid-treated astrocytes, consistent with depletion of substrate supply or damage to the respiratory chain. DPQ (20 μM) prevented the effect of β-amyloid, restoring both resting and FCCP-induced oxygen consumption in β-amyloid-treated astrocytes. *$P < 0.05$ vs blank control.

value (Fig. 2A). Thus, a combination of measurements using NaCN and FCCP allows an estimate of the full dynamic range of the signal (see 'Materials and methods' section). A high concentration of glutamate (1 mM), which we have previously shown prevented the slow depolarization (Abramov *et al.*, 2004*a*), increased NADH autofluorescence in hippocampal astrocytes by 12.1 ± 0.7% and greatly reduced the effect of β-amyloid on NAD(P)H fluorescence (showing a decrease of only 14.5 ± 0.9%, $n = 99$ compared with 32 ± 2.1% in astrocytes without glutamate pretreatment, $n = 101$, $P < 0.05$) (Fig. 2B). Interestingly, activation of the NAD(P)H oxidase by PMA (1 μg/ml), which we have shown in Fig. 1B induces mitochondrial depolarization in astrocytes, also decreased NADH autofluorescence by 22.3 ± 4.2% ($n = 47$; data not shown).

The enzyme PARP-1, a nuclear protein that plays a role in DNA repair and which is activated by DNA strand breaks triggered by free radical species, may consume NAD^+ and so cause a loss of mitochondrial membrane potential by depletion of respiratory substrate (Du *et al.*, 2003; Abramov and Duchen, 2008). Pre-incubation of primary hippocampal co-cultures with the inhibitors of PARP, DPQ (20 μM; Fig. 2C) or 3-aminobenzamide (1 mM; data not shown), significantly reduced the effect of β-amyloid on the NAD(P)H autofluorescence signal. Thus, NAD(P)H autofluorescence decreased by only 12.6 ± 1.1% after 20 min of exposure to β-amyloid$_{1–42}$ in cells pretreated with DPQ ($n = 64$ cells, $n = 3$ experiments) and by 14.8 ± 0.9% with 3-aminobenzamide ($n = 121$ cells, $n = 3$ experiments) compared with a decrease of 32 ± 2.1% in control cells ($P < 0.001$; Fig. 2C).

β-amyloid decreases oxygen consumption in cortical astrocytes

A decrease in NADH autofluorescence coupled with a loss of mitochondrial membrane potential could reflect an increased mitochondrial leak and uncoupling (i.e. the loss of potential drives an increased respiratory rate and therefore an increased rate of oxidation of the NADH pool) or a lack of substrate (i.e. the decrease in NADH supply is primary, fails to support respiration and so the mitochondrial depolarization is secondary to a loss of substrate availability). In the former, oxygen consumption would be increased; in the latter case, it would be decreased. Measurements of oxygen consumption (Fig. 2D) showed that basal oxygen consumption was significantly reduced 5–7 min after exposure to 50 μM β-amyloid$_{25–35}$ compared with control values of 1.1 ± 0.09 nmol/O_2/min/10^6 cells, $n = 3$ experiments to 0.72 ± 0.05 nmol/O_2/min/10^6 cells ($n = 4$ experiments, $P < 0.05$). Maximal respiratory capacity was assessed by addition of 0.5 μM FCCP, which accelerated respiration to 4.27 ± 0.39 nmol/O_2/min/10^6 in control cells (Fig. 2D). After exposure to β-amyloid, maximal FCCP-induced respiration was reduced to only 3.01 ± 0.22 nmol/O_2/min/10^6 cells ($n = 3$; $P < 0.05$). Pre-incubation of primary hippocampal astrocytes with the PARP inhibitor DPQ (20 μM) prevented the β-amyloid-induced inhibition of respiration (Fig. 2D, $n = 3$ experiments). Thus, the basal rate of respiration, measured after 10 min 50 μM β-amyloid$_{25–35}$ exposure in the presence of DPQ, and the maximal FCCP stimulated respiration, did not show significant differences when compared with control (basal 1.35 ± 0.11 nmol/O_2/min/10^6 cells; FCCP 3.45 ± 0.28 nmol/O_2/min/10^6 cells; $n = 3$ experiments; Fig. 2D). These data are consistent with a generalized inhibition of respiration by β-amyloid through activation of PARP-1, consistent with rate-limiting substrate availability.

Our previous data suggested that the progressive mitochondrial depolarization reflects a progressive loss of substrate as $\Delta\psi_m$ could be preserved with pyruvate, methyl succinate or TMPD/ascorbate (Abramov *et al.*, 2004*a*). Similarly, the PARP inhibitors DPQ and 3-aminobenzamide not only limited the β-amyloid-induced NAD(P)H depletion and restored oxygen consumption, but also prevented the β-amyloid-induced slow mitochondrial depolarization. Thus, pre-incubation of primary hippocampal co-cultures with DPQ (20 μM) or 3-aminobenzamide (1 mM), 20 and 10 min, respectively, completely prevented the slow mitochondrial depolarization in astrocytes ($n = 187$ for DPQ, $n = 167$ for 3-aminobenzamide) but had no effect on either the β-amyloid-induced $[Ca^{2+}]_c$ signals or the large transient mitochondrial depolarizations (Fig. 3A; 3-aminobenzamide—data not shown). Interestingly, the PARP-1 inhibitors also abolished the loss of $\Delta\psi_m$ induced by PMA (1 μg/ml) (Fig. 3B). In experiments with hippocampal astrocytes cultured from transgenic cyclophilin D knockout mice, in which the transient depolarizations were absent, pretreatment with 3-aminobenzamide (1 mM) completely prevented all mitochondrial responses to 5 μM β-amyloid$_{1–42}$, while the $[Ca^{2+}]_c$ signal was unaffected ($n = 98$; Fig. 3C).

β-amyloid causes overactivation of PARP-1 in astrocytes

PARP-1 activity generates PAR polymers, accounting for >99% of PAR synthesis in the cell during genotoxic stress (for review see Heeres and Hergenrother, 2007). We used an anti-PAR antibody (a kind gift from Matthias Ziegler, University of Bergen) to estimate PARP-1 activity using immunofluorescence in astrocytes following exposure to β-amyloid. In untreated cells, no specific signal could be detected above background (Fig. 4A). Application of β-amyloid$_{1–42}$ (5 μM) or 25–35 (50 μM) for 1 h clearly caused accumulation of PAR in glial fibrillary acidic protein-positive cells (i.e. astrocytes), $n = 42$ cells for control; $n = 56$ for β-amyloid (Fig. 4A, B). The NADPH oxidase inhibitor diphenylene iodonium (0.5 μM) significantly reduced the effect of β-amyloid on PAR accumulation in astrocytes (mean values of PAR-fluorescence decreased by 71.8%, $n = 37$ Fig. 4C). Increased α-PAR staining was not detectable in neurons ($n = 58$ for control; $n = 32$ for β-amyloid; Fig. 4D). The specificity of the experiment as an assay of PARP activity was confirmed using the PARP inhibitor, 3-aminobenzamide, which also significantly inhibited the effect of β-amyloid in astrocytes (by 73%; $n = 48$, $P < 0.001$).

Chronic exposure to β-amyloid depletes the NADH pool of hippocampal neurons

One hour exposure of β-amyloid did not induce PARP-1 activation or mitochondrial depolarization in neurons. However, more prolonged exposure to the peptide over 24 h caused substantial

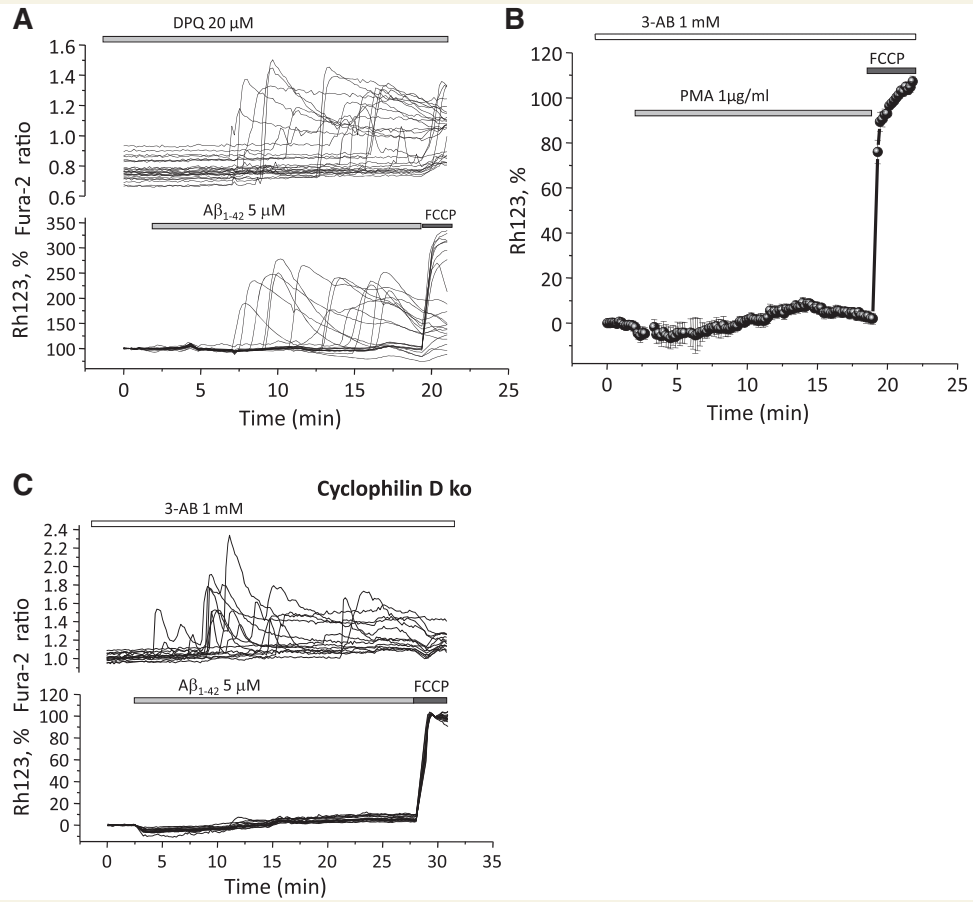

Figure 3 PARP-1 drives mitochondrial depolarization induced by β-amyloid following activation of the NADPH oxidase. (**A**) Inhibitors of PARP-1, DPQ (20 μM) or 3-aminobenzamide (3-AB) (1 mM) blocked the slow mitochondrial depolarization induced by exposure to β-amyloid$_{1–42}$ (5 μM) in wild-type astrocytes. (**B**) The mitochondrial depolarization induced by PMA was also prevented by PARP inhibitors—illustrated here for (3-AB) (1 mM). (**C**) In hippocampal astrocytes from cyclophilin D knockout mice, addition of the PARP inhibitor 3-AB prevented any significant loss of mitochondrial membrane potential in response to Aβ$_{1–42}$.

neuronal death with only a small increase in astrocytic death (Abramov *et al.*, 2004*a*). We therefore explored the role of PARP-1 in neurons during prolonged (24 h) exposure to β-amyloid. The mitochondrial membrane potential, the NADH pool and the redox index were measured as described in the 'Materials and methods' section, at a series of time points over 24 h of exposure to 5 μM β-amyloid$_{1–42}$. The mitochondrial NADH pool (Fig. 5A) was estimated by identifying the difference in the values of fluorescence between application of FCCP when the NADH signal is maximally oxidized and of NaCN, when the pool is maximally reduced (Fig. 5A). $\Delta\psi_m$ in neurons did not change significantly (only to 89.4 ± 7.2% of basal, $n = 20$; Fig. 5B) over up to 8 h of exposure to β-amyloid. However, the mean values of $\Delta\psi_m$ were significantly reduced after more prolonged (15 h) β-amyloid exposure, reaching 44.4 ± 5.6% ($n = 27$ cells; $P < 0.001$) of control values. After 24 h, $\Delta\psi_m$ was further reduced to just 22.4 ± 1.9% of the basal value ($n = 21$; $P < 0.001$). The loss of $\Delta\psi_m$ was preceded by depletion of the NADH pool, which started to decrease ~4 h after application of β-amyloid (at 91.5 ± 5.1% of basal, $n = 26$), accompanied by a small oxidation of the pool from a resting value of 56.7 ± 5.1% ($n = 29$) to 48.4 ± 2.7% (Fig. 5B). The NADH pool decreased progressively throughout the 24 h following β-amyloid exposure resulting in a decrease of 71.3 ± 2% after 24 h, $n = 35$; $P < 0.001$. The redox state also showed a progressive oxidation from a value of 56.7 ± 5.1% to a final level of just 27.8 ± 1.7% at 24 h ($P < 0.001$; Fig. 5B), consistent with the idea that the NADH pool was rate limiting as the remaining NADH became more oxidized. The changes in the NADH pool were prevented by PARP-1 inhibitors, measured at 24 h. Thus, the β-amyloid induced decrease in the NADH pool was significantly reduced in the presence of DPQ or 3-aminobenzamide (by 45.5 ± 1.3%, $P < 0.05$ for DPQ and by 43.7 ± 3.57%, $P < 0.05$ for 3-aminobenzamide compared with 71.3 ± 2% for β-amyloid$_{1–42}$ only; Fig. 5C), supporting the role of PARP-1 in this process. Thus, prolonged exposure to β-amyloid induced activation of PARP-1 not only in astrocytes but also in neurons, and promoted neuronal death.

β-amyloid exposure impairs glucose uptake in astrocytes

The slow mitochondrial depolarization, induced by β-amyloid exposure, can either be prevented or reversed by providing mitochondrial substrates at all parts of the respiratory chain—from

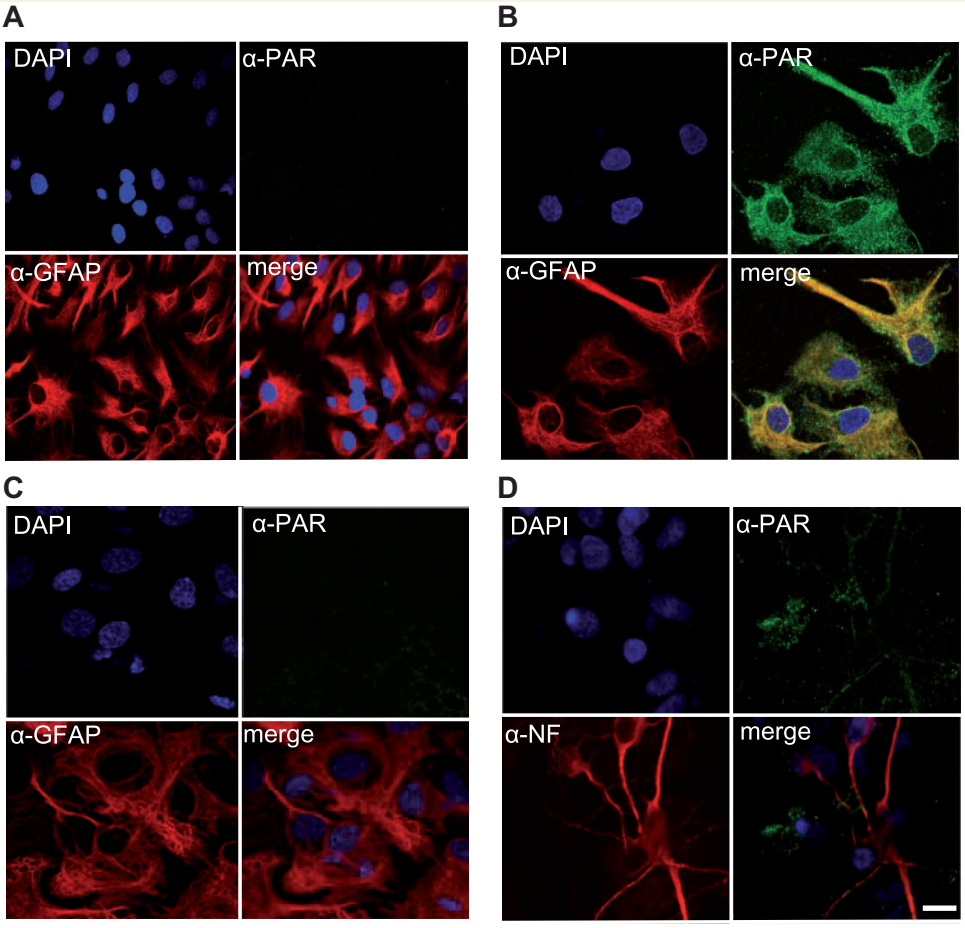

Figure 4 β-amyloid increases production of PAR polymers in astrocytes. (**A–D**) Immunofluorescence images of PAR (FITC; green) co-stained with anti-glial fibrillary acidic protein (GFAP) (Cy3; red **A–C**) or anti-neurofilament (NF) (Cy3; red **D**) and DAPI (blue) shows the presence of PAR polymers in astrocytes treated with β-amyloid$_{25–35}$ (50 μM) for 1 h at 37°C. No PAR staining was seen in adjacent neurons in the co-cultures (**D**). The generation of PAR polymers was prevented by pre-incubation of the cultures with the inhibitor of the NADPH oxidase, diphenylene iodonium (DPI) (**C**) (0.5 μM, added 20 min before and during exposure to β-amyloid$_{25–35}$). Scale bars = 20 μm.

pyruvate at complex I to TMPD/ascorbate at complex IV (Abramov *et al.*, 2004*a*, 2005), implying impaired substrate supply upstream of pyruvate. The data we have shown so far suggest that PARP-1 activation plays a major role in depletion of NAD^+ leading to depletion of substrate supply. However, oxidative stress alone can impair glucose uptake (Andreoli *et al.*, 1993), which might contribute to impaired substrate delivery. We therefore measured the rate of glucose uptake in primary co-cultures of neurons and astrocytes using a fluorescent analogue of glucose, 2-NBDG (2 μM). These experiments clearly showed that both the full peptide β-amyloid$_{1–42}$ (5 μM) and the peptide fragment β-amyloid$_{25–35}$ (50 μM) significantly and acutely reduced the rate of glucose uptake (Fig. 6A–B). β-amyloid decreased the rate of glucose uptake not only in astrocytes but also in neurons in the same co-cultures. Thus, in astrocytes 50 μM β-amyloid$_{25–35}$ reduced the rate of increase of intracellular 2-NBDG fluorescence to 62.7 ± 2.7% of controls ($n = 96$ cells; $n = 4$ experiments) and 5 μM β-amyloid$_{1–42}$ reduced it to 59.8 ± 4.1% ($n = 87$ cells; $n = 4$ experiments; $P < 0.05$ for both conditions), while the rate of uptake in neurons was also reduced to 67.4 ± 3.8% by β-amyloid$_{25–35}$ ($n = 63$ cells; $n = 3$ experiments) and to 65.7 ± 4% by β-amyloid$_{1–42}$ ($n = 59$ cells; $n = 3$ experiments; $P < 0.05$ for both conditions), respectively.

Role of PARP in β-amyloid-induced neuronal death

To corroborate our previous data we examined the effect of 24 h exposure of cultures to β-amyloid$_{25–35}$ on cell viability with or without PARP-1 inhibitors. Neurons (29 ± 0.83%) and 9.05 ± 3.3% of astrocytes died in this period in hippocampal co-cultures (Fig. 6C; $n = 3$ experiments). Pre-incubation of co-cultures with the PARP-1 inhibitor DPQ (20 μM) significantly reduced cell death of hippocampal neurons to 5.31 ± 0.32%, $P < 0.05$ ($n = 3$ experiments; Fig. 6C). DPQ had no effect on cell death in astrocytes. The presence or absence of DPQ in the medium did not significantly change the percentage of dead cells

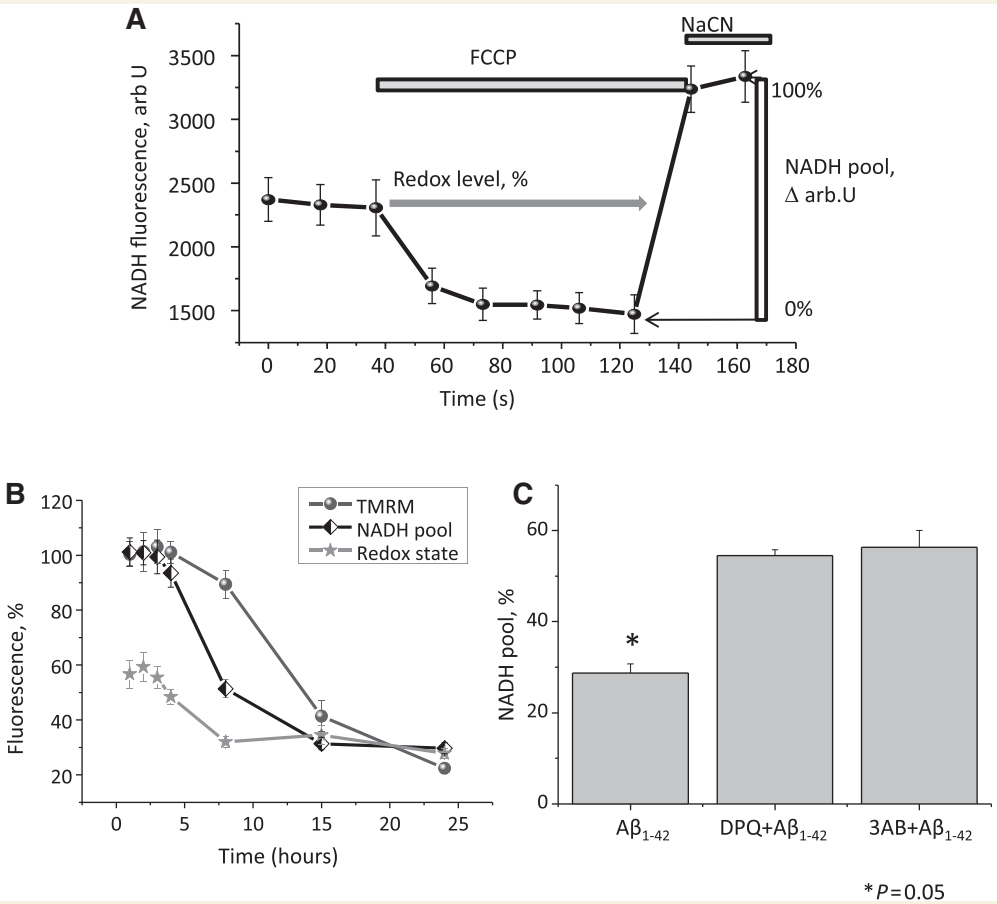

Figure 5 β-amyloid causes PARP-1 dependent NADH depletion, mitochondrial depolarization. (**A**) The method used to measure the fluorescence signal derived from the total mitochondrial NADH pool. NADH fluorescence was measured from individual astrocytes. Application of FCCP drives mitochondrial respiration to maximum and causes maximal oxidation of the mitochondrial NADH pool. Subsequent addition of CN^- inhibits respiration, prevents NADH oxidation and so the mitochondrial NADH pool becomes maximally reduced to yield a maximum fluorescence signal. The signals were therefore normalized between 0, the response to 1 μM FCCP, and 100%, the response to cyanide. The resting level was then defined as the redox index. The total NADH pool was estimated from the same experiments as the difference between responses to FCCP and CN^-. (**B**) Mitochondrial membrane potential and NADH signals were measured in neurons over a range of time points during 24 h exposure of 5 μM β-amyloid$_{1–42}$. β-amyloid caused a significant oxidation of NADH and a decrease in the apparent mitochondrial NADH pool, followed by the progressive loss of $\Delta\psi_m$, measured as the mean mitochondrial TMRM fluorescence signal. These changes were prevented by incubation of cells with the PARP-1 inhibitors DPQ (20 μM) or 3-aminobenzamide (3AB, 1 mM), represented in the histogram in (**C**), which shows measurements of the NADH pool in cells incubated for 24 h with β-amyloid$_{1–42}$ with and without the PARP-1 inhibitors 3-aminobenzamide and DPQ (the control was taken as 100%). *$P < 0.05$.

in untreated co-cultures (Fig. 6C). These experiments confirm that PARP-1 plays a key role in β-amyloid-induced neuronal death.

Overactivation of PARP-1 in a transgenic Alzheimer mouse model

Although PAR polymers did not seem to be present in neurons after 1 h of β-amyloid incubation, we found that PARP-1 inhibitors protect neurons from both NAD^+ depletion and cell death during 24 h of β-amyloid exposure. In light of these results, we sought evidence for activation of PARP-1 in the CNS of a transgenic Alzheimer mouse model. To this purpose, we carried out immunofluorescence studies for PAR polymers in brain sections from a double transgenic mouse model known as the TASTPM mouse, which carries both the human APP and Presenilin 1 mutations, (Howlett *et al.*, 2004). This mouse model presents significant cognitive impairment at just 4 months old, becoming more severe at 8 months of age. PAR polymers were clearly demonstrable in fixed sections from the mice, increasing with age. Figure 7A(a) shows a section labelled with α-MAP-2 (for neurons) and α-PAR (for PAR polymers) in wild-type mice and on the right, Fig. 7A(b) shows a section of 4-month-old TASTPM. PAR polymers were widely present in material from the TASTPM mice and absent in wild-type neurons and astrocytes. Fig. 7A(c) shows a parallel experiment, using α-glial fibrillary acidic protein to label astrocytes, again showing significant PAR immunorectivity in the transgenic animal. In order to assess whether the amyloid plaques were present in

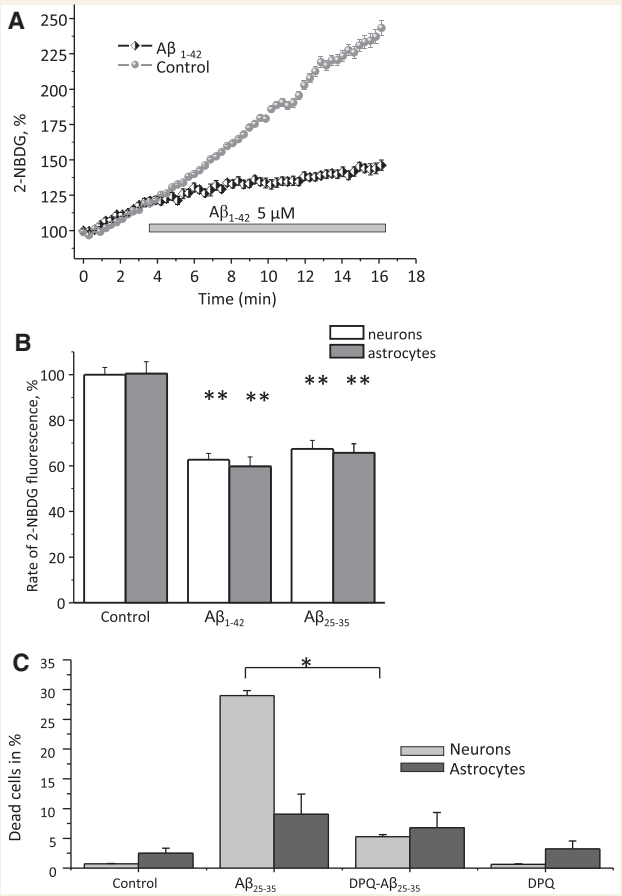

Figure 6 β-amyloid impairs the rate of glucose uptake in neurons and astrocytes and PARP-1 dependent cell death in neurons. Measurement of cellular fluorescence from 2-NBDG, a fluorescent analogue of glucose, in order to assess the rate of glucose uptake revealed that β-amyloid$_{1–42}$ (5 μM) and β-amyloid$_{25–35}$ (50 μM) caused a rapid decrease in the rate of glucose uptake in hippocampal astrocytes (**A, B**) and in neurons (**B**). (**C**) Propidium iodide and Hoechst fluorescence were used to detect cell death after 24 h exposure to 50 μM β-amyloid$_{25–35}$ (Aβ). Dead cells (labelled with propidium iodide) were counted with respect to the total number of cells present, identified by staining the nuclei with Hoechst 33342 and using the phase contrast image to distinguish neurons and astrocytes. β-amyloid increased cell death significantly in neurons but caused only a modest increase in astrocyte cell death. The PARP inhibitor DPQ significantly reduced β-amyloid-induced neuronal cell death. $^*P < 0.05$.

mice at 4 and 8 months old, we labelled the tissue with a specific antibody against β-amyloid. Plaques were apparent in mice at 4 months of age, and were widespread by 8 months of age (data not shown). These data suggest that in the mouse model in which amyloid is forming plaques, PARP-1 is activated with accumulation of PAR polymers. In Fig. 7B, the intensity profile across a neuron is highlighted to show the appearance of PAR polymers in a neuron at this stage of the disease (8 months). To corroborate our data we have sought evidence for long-term increased activation of the NADPH oxidase in the TASTPM mice compared with matched littermate controls. We have therefore carried out western blot analysis of the phosphorylated form of p40phox, a cytosolic subunit of the NADPH oxidase that is phosphorylated and translocates to the plasma membrane on activation (Bouin *et al.*, 1998). We found a highly significant increase in the presence of phosphorylated p40phox at 4 months that increased further at 8 months in the cortex of the TASTPM mice (Fig. 8). These data, together with the rest of the data presented in this study, lend further support to the hypothesis that activation of the NADPH oxidase underlies the activation of PARP-1 and the generation of PAR polymers in the Alzheimer's disease brain.

Discussion

We have demonstrated here that the overactivation of PARP-1 in astrocytes results in the depletion of mitochondrial substrate and mitochondrial depolarization. The critical events leading to PARP-1 overactivation involve the activation of the NADPH oxidase which generates oxidative stress, seen as an increase in the rate of reactive oxygen species generation and glutathione depletion (Abramov *et al.*, 2004*a*). Remarkably, the astrocytes seem able to withstand these conditions and do not die. We have previously shown that neurons in co-culture with the astrocytes also become glutathione depleted and that they can be protected by antioxidants, by inhibition of the NADPH oxidase and by provision of glutathione precursors, suggesting that the neuronal death that follows after 24 h of exposure is a result of the oxidative stress initiated by the glial NADPH oxidase (Abramov *et al.*, 2004*a, b*). In the current study, we have found that the neuronal cell death results from the overactivation of PARP-1 leading to loss of $\Delta\psi_m$ in the neurons. While increased levels of PARP-1 expression and accumulation of PAR polymers have been demonstrated in the brains and peripheral cells of patients with Alzheimer's disease (Love *et al.*,1999; Cecchi *et al.*,2002), this is the first description, to our knowledge, of the role of PARP-1 in the mechanism of β-amyloid-induced neurotoxicity.

In this study, we have described unusually complex changes in mitochondrial potential in astrocytes following exposure to β-amyloid. These involved a slowly progressive loss of potential over about an hour, and superimposed on this slow response were transient and reversible depolarizations. Our data strongly suggest roles for two different processes, both of which represent responses to oxidative stress. We now propose that the slow progressive loss of potential results from the depletion of NAD^+ by overactivation of PARP-1, while the transient depolarizations reflect apparently reversible openings of the mitochondrial permeability transition pore—they are calcium dependent, they are prevented by cyclosporin A (Abramov *et al.*, 2004*a*, *b*, 2007*b*) and we have now also shown that they are absent in cells derived from the cyclophilin D knockout mouse. To our surprise, all our data suggest that reversible mitochondrial permeability transition pore openings play a very small role in driving cell death in this model. However, inhibition of β-amyloid-induced mitochondrial permeability transition pore opening using a variety of different approaches, in the presence of cyclosporin A, or in cyclophilin D knockout astrocytes or by depletion of polyphosphate from mitochondria (which prevents Ca^{2+}-dependent mitochondrial

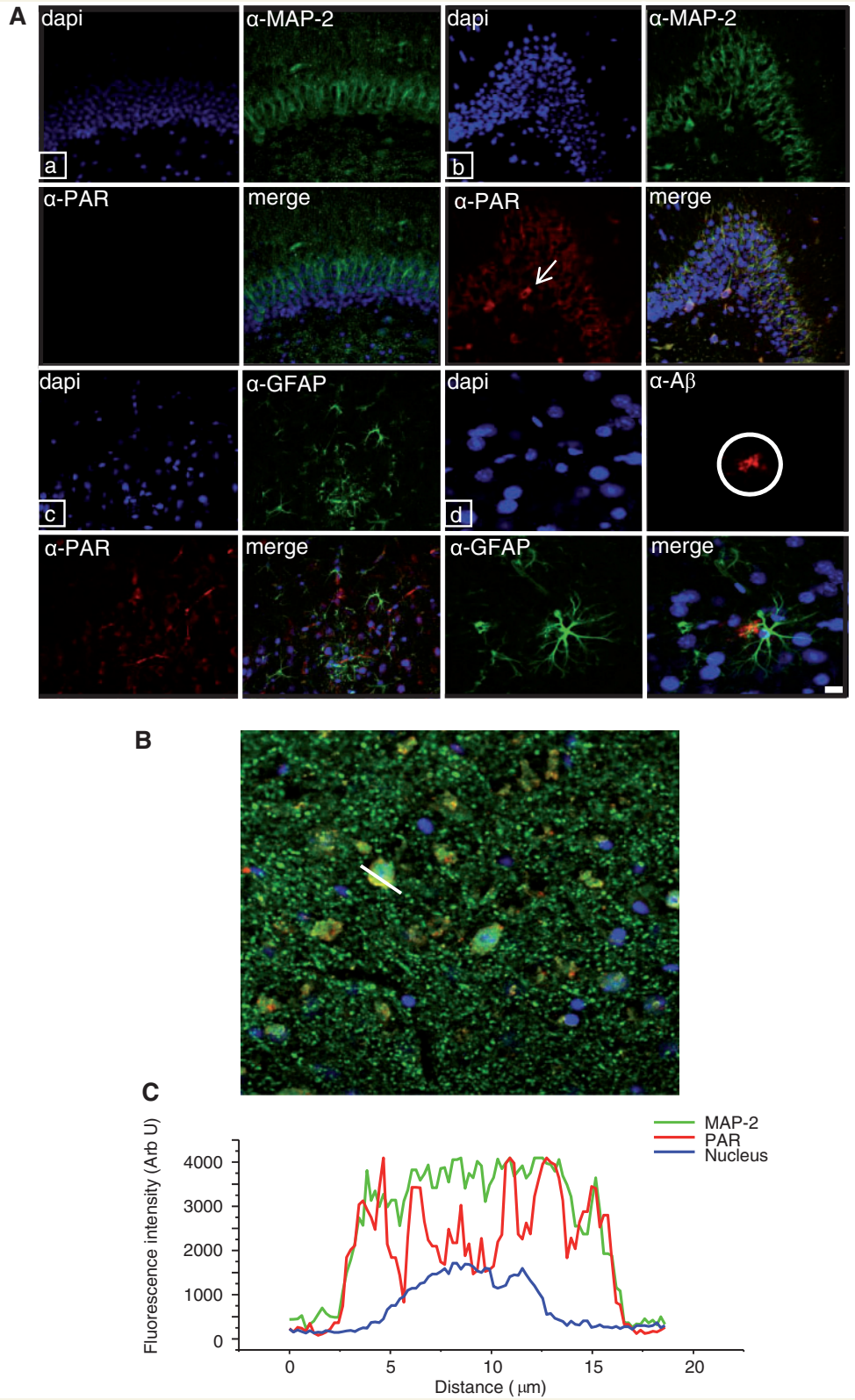

Figure 7 PAR polymers are present and increase with age in the TASTPM transgenic Alzheimer's disease mouse model. (**A**) Immunofluorescence for PAR polymers in tissue sections from a control (**a**) and from the TASTPM mouse at 4 months (**b**) and 8 months (**c**) of age. Nuclei are stained with DAPI (blue), α-MAP-2 (green) was used to label neurons and α-glial fibrillary acidic protein (GFAP) to label astrocytes. The presence of PAR polymers in the TASTPM tissue is evident (white arrow). (**Ad**) The presence of β-amyloid deposits as plaques in the TASTPM tissue (α- β-amyloid, red). (**B**) A merged image of the staining of a section from an 8-month-old TASTPM mouse for α-MAP-2, α-PAR and DAPI. (**C**) Intensity profile along the line indicated to demonstrate the colocalization of PAR polymers (red) and the neuronal marker, MAP-2 (green), revealing that PARs are present in the cell body of the neuron. Scale bars = 20 μm.

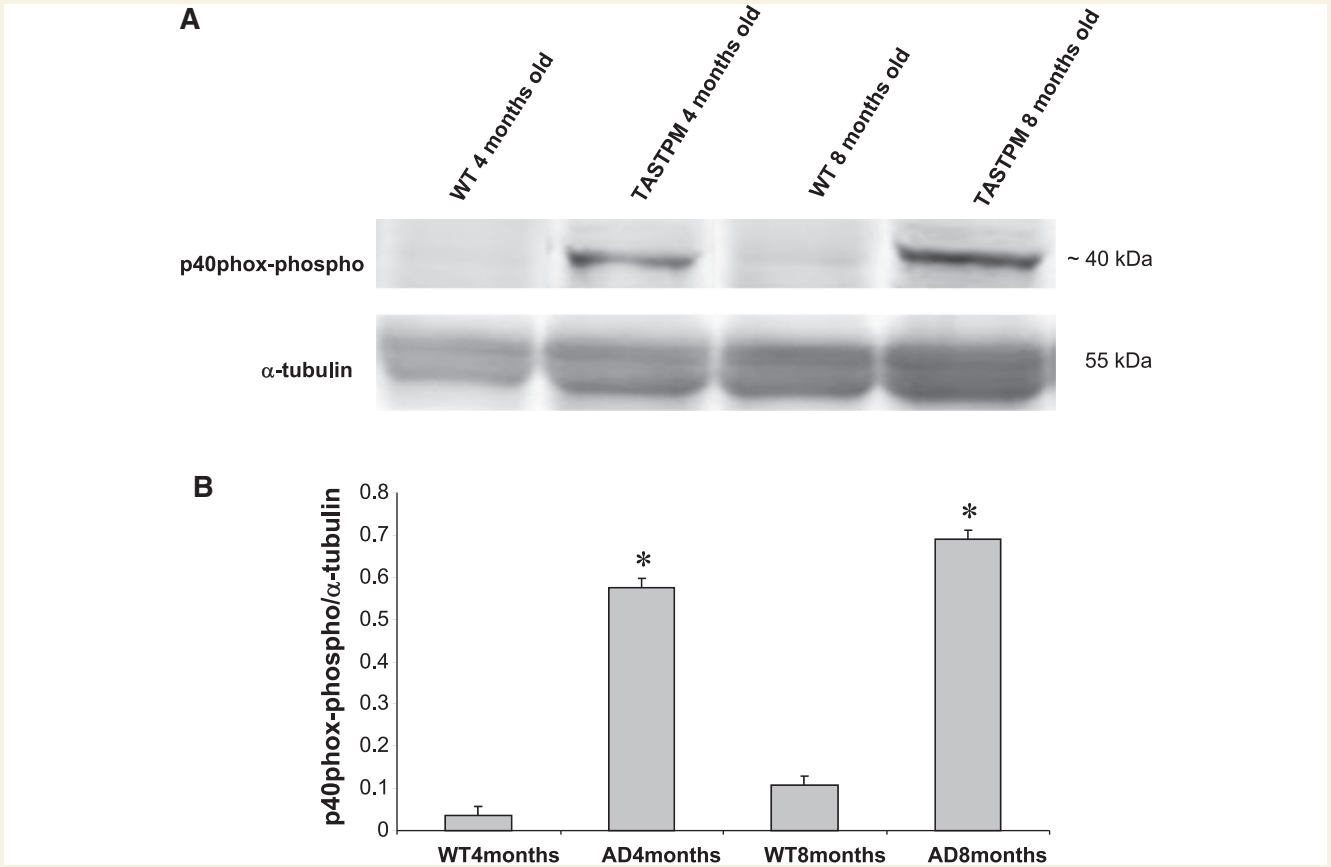

Figure 8 NADPH oxidase activation in the TASTPM transgenic Alzheimer's disease mouse model. (**A**) Brain samples from wild-type (WT) and TASTPM mice at 4 and 8 months old were resolved in sodium dodecyl sulphate polyacrylamide gel electrophoresis and transferred into nitrocellulose membrane, where phosphorylated p40phox and α-tubulin were labelled. (**B**) The level of phosphorylated p40phox normalized against α-tubulin, in three different blots; $^{*}P = 0.05$.

permeability transition pore opening) (Abramov *et al.*, 2007) significantly increased the rate of the 'slow' mitochondrial depolarization, suggesting that the mitochondrial permeability transition pore or its components may play a role, as yet unidentified, in limiting the impact of substrate depletion.

The role of PARP-1 in the response seems clearly established—loss of $\Delta\psi_m$ in astrocytes was accompanied by a reduction in NADH and by a decrease in the rate of oxygen consumption, suggesting that the primary event is NAD^+ depletion while the loss of $\Delta\psi_m$ is secondary. These physiological changes were accompanied by an increase in the presence of PAR polymers in the astrocytes. Several observations presented here suggest that PARP-1 depletes the cytosolic NAD^+ pool, and there is no need to argue either for access of nuclear PARP-1 to the mitochondrial NAD^+ pool or for a role for intra-mitochondrial PARP (Du *et al.*, 2003). It has been suggested that mitochondrial permeability transition pore opening gives PARP-1 access to mitochondrial NAD^+ (Alano *et al.*, 2004). However, this is apparently not required to account for our current observations, as the slow mitochondrial depolarization still occurred (and was abolished by PARP-1 inhibitors) in the cyclophilin D knockout astrocytes in which the mitochondrial permeability transition pore is largely suppressed. Remarkably, while the NADH autofluorescence signal declined dramatically in the presence of β-amyloid, it was almost completely maintained even in the presence of the complex I substrates, pyruvate or glutamate. This would not be possible if the mitochondrial NAD^+ pool were depleted by PARP, and yet the NADH signal, which mostly derives from mitochondrial NADH, is clearly almost maximally oxidized, as shown by the very small decrease in signal caused by FCCP. Therefore, this mode of imaging the instrinsic fluorophore NADH reveals that PARP-1 must act primarily to deplete cytosolic NAD^+, which will largely inhibit glycolysis. This in turn will limit the provision of pyruvate so that the mitochondrial NADH pool becomes progressively oxidized. This explains the remarkably protective effect of pyruvate and the dramatic increase in (or preservation of) the NADH signal on provision of mitochondrial complex I substrates.

The modulation of glucose uptake during Alzheimer's disease pathology has been previously observed and is a feature of the Alzheimer's disease transgenic mouse models (Keller *et al.*,1997; Parpura-Gill *et al.*,1997; Uemura and Greenlee, 2001), so we explored the effect of β-amyloid on glucose uptake in the cell model. Measurements of the rate of accumulation of the fluorescent glucose analogue 2-NBDG showed that exposure to β-amyloid clearly decreased the glucose uptake rate. However, the action of the peptide on the rate of 2-NBDG fluorescence

was almost immediate, while there is typically a delay of ~5–10 min before β-amyloid induces calcium signals or reactive oxygen species generation in astrocytes. Therefore, it seems unlikely that this phenomenon should be induced by reactive oxygen species production from NADPH oxidase, but more likely to be explained by a direct action of β-amyloid on glucose transporters. This particular effect did not seem to play a major role in the pathophysiology, as inhibition of PARP-1 alone or in combination with cyclosporin A almost completely abolished neuronal death induced by β-amyloid.

Finally, the striking presence of PAR polymers in both neurons and astrocytes in brain sections from the TASTPM Alzheimer's disease mice emphasizes the relevance of our experiments and strongly support a role for PARP-1 overactivation in Alzheimer's disease, corroborated by the demonstration of the long-term activation of the NADPH oxidase complex in the TASTPM mouse brain.

In summary, our data strongly implicate major roles for the glial NADPH oxidase and resultant oxidative stress as a trigger for β-amyloid-induced neuronal death, suggesting that death is executed by the metabolic failure that follows overactivation of PARP-1, raising new questions in the field and suggesting several potentially important therapeutic targets in the search for better management of Alzheimer's disease.

Acknowledgements

We thank Glaxo Smith Kline for giving us access to the TASTPM mice, which is a strain generated at Glaxo Smith Kline, and Damian Cummings for providing them to us.

Funding

UCL studentship (to R.A.).

References

Abramov AY, Canevari L, Duchen MR. Changes in intracellular calcium and glutathione in astrocytes as the primary mechanism of amyloid neurotoxicity. J Neurosci 2003; 23: 5088–95.

Abramov AY, Canevari L, Duchen MR. Beta-amyloid peptides induce mitochondrial dysfunction and oxidative stress in astrocytes and death of neurons through activation of NADPH oxidase. J Neurosci 2004a; 24: 565–75.

Abramov AY, Canevari L, Duchen MR. Calcium signals induced by amyloid beta peptide and their consequences in neurons and astrocytes in culture. Biochim Biophys Acta 2004b; 1742: 81–7.

Abramov AY, Duchen MR. Mechanisms underlying the loss of mitochondrial membrane potential in glutamate excitotoxicity. Biochim Biophys Acta 2008; 1777: 953–64.

Abramov AY, Fraley C, Diao CT, Winkfein R, Colicos MA, Duchen MR, et al. Targeted polyphosphatase expression alters mitochondrial metabolism and inhibits calcium-dependent cell death. Proc Natl Acad Sci USA 2007; 104: 18091–6.

Abramov AY, Jacobson J, Wientjes F, Hothersall J, Canevari L, Duchen MR. Expression and modulation of an NADPH oxidase in mammalian astrocytes. J Neurosci 2005; 25: 9176–84.

Alano CC, Ying W, Swanson RA. Poly(ADP-ribose) polymerase-1-mediated cell death in astrocytes requires NAD+ depletion and mitochondrial permeability transition. J Biol Chem 2004; 279: 18895–902.

Andreoli SP, McAteer JA, Seifert SA, Kempson SA. Oxidant-induced alterations in glucose and phosphate transport in LLC-PK1 cells: mechanisms of injury. Am J Physiol 1993; 265: F377–84.

Baines CP, Kaiser RA, Purcell NH, Blair NS, Osinska H, Molkentin D, et al. Loss of cyclophilin D reveals a critical role for mitochondrial permeability transition in cell death. Nature 2005; 434: 658–62.

Blass JP, Gibson GE. The role of oxidative abnormalities in the pathophysiology of Alzheimer's disease. Rev Neurol 1991; 147: 513–25.

Bouin AP, Grandvaux N, Vignais PV, Fuchs A. p40(phox) is phosphorylated on threonine 154 and serine 315 during activation of the phagocyte NADPH oxidase. Implication of a protein kinase c-type kinase in the phosphorylation process. J Biol Chem 1998; 273: 30097–103.

Burkle A. Poly(ADP-ribose). The most elaborate metabolite of NAD+. FEBS J 2005; 272: 4576–89.

Casley CS, Canevari L, Land JM, Clark JB, Sharpe MA. Beta-amyloid inhibits integrated mitochondrial respiration and key enzyme activities. J Neurochem 2002; 80: 91–100.

Cecchi C, Fiorillo C, Sorbi S, Latoracca S, Nacmias B, Bagnoli S, et al. Oxidative stress and reduced antioxidant defenses in peripheral cells from familial Alzheimer's patients. Free Radic Biol Med 2002; 33: 1372–9.

Chance B. Pyridine nucleotide as an indicator of the oxygen requirements for energy-linked functions of mitochondria. Circ Res 1976; 38: I31–8.

Crompton M, Barksby E, Johnson N, Capano M. Mitochondrial intermembrane junctional complexes and their involvement in cell death. Biochimie 2002; 84: 143–52.

Diefenbach J, Burkle A. Introduction to poly(ADP-ribose) metabolism. Cell Mol Life Sci 2005; 62: 721–30.

Du L, Zhang X, Han YY, Burke NA, Kochanek PM, Watkins SC, et al. Intra-mitochondrial poly(ADP-ribosylation) contributes to NAD+ depletion and cell death induced by oxidative stress. J Biol Chem 2003; 278: 18426–33.

Hardy J, Selkoe DJ. The amyloid hypothesis of Alzheimer's disease: progress and problems on the road to therapeutics. Science 2002; 297: 353–6.

Heeres JT, Hergenrother PJ. Poly(ADP-ribose) makes a date with death. Curr Opin Chem Biol 2007; 11: 644–53.

Hirai K, Aliev G, Nunomura A, Fujioka H, Russell RL, Atwood CS, et al. Mitochondrial abnormalities in Alzheimer's disease. J Neurosci 2001; 21: 3017–23.

Howlett DR, Richardson JC, Austin A, Parsons AA, Bate ST, Davies DC, et al. Cognitive correlates of Abeta deposition in male and female mice bearing amyloid precursor protein and presenilin-1 mutant transgenes. Brain Res 2004; 1017: 130–6.

Keller JN, Pang Z, Geddes JW, Begley JG, Germeyer A, Waeg G, et al. Impairment of glucose and glutamate transport and induction of mitochondrial oxidative stress and dysfunction in synaptosomes by amyloid beta-peptide: role of the lipid peroxidation product 4-hydroxynonenal. J Neurochem 1997; 69: 273–84.

Love S, Barber R, Wilcock GK. Increased poly(ADP-ribosyl)ation of nuclear proteins in Alzheimer's disease. Brain 1999; 122 (Pt 2): 247–53.

Masters CL, Multhaup G, Simms G, Pottgiesser J, Martins RN, Beyreuther K. Neuronal origin of a cerebral amyloid: neurofibrillary tangles of Alzheimer's disease contain the same protein as the amyloid of plaque cores and blood vessels. EMBO J 1985; 4: 2757–63.

Moroni F. Poly(ADP-ribose)polymerase 1 (PARP-1) and postischemic brain damage. Curr Opin Pharmacol 2008; 8: 96–103.

Parks JK, Smith TS, Trimmer PA, Bennett JP Jr, Parker WD Jr. Neurotoxic Abeta peptides increase oxidative stress in vivo through NMDA-receptor and nitric-oxide-synthase mechanisms, and inhibit complex IV activity and induce a mitochondrial permeability transition in vitro. J Neurochem 2001; 76: 1050–6.

Parpura-Gill A, Beitz D, Uemura E. The inhibitory effects of beta-amyloid on glutamate and glucose uptakes by cultured astrocytes. Brain Res 1997; 754: 65–71.

Pelech SL. Networking with proline-directed protein kinases implicated in tau phosphorylation. Neurobiol Aging 1995; 16: 247–56.

Rasola A, Bernardi P. The mitochondrial permeability transition pore and its involvement in cell death and in disease pathogenesis. Apoptosis 2007; 12: 815–33.

Sheehan JP, Swerdlow RH, Miller SW, Davis RE, Parks JK, Parker WD, et al. Calcium homeostasis and reactive oxygen species production in cells transformed by mitochondria from individuals with sporadic Alzheimer's disease. J Neurosci 1997; 17: 4612–22.

Shevtzova EF, Kireeva EG, Bachurin SO. Effect of beta-amyloid peptide fragment 25-35 on nonselective permeability of mitochondria. Bull Exp Biol Med 2001; 132: 1173–6.

Uemura E, Greenlee HW. Amyloid beta-peptide inhibits neuronal glucose uptake by preventing exocytosis. Exp Neurol 2001; 170: 270–6.

Wilcock GK, Esiri MM. Plaques, tangles and dementia. A quantitative study. J Neurol Sci 1982; 56: 343–6.